

# Aging in a simple glassformer<sup>1</sup>

Walter Kob<sup>+</sup>, Jean-Louis Barrat<sup>†</sup>, Francesco Sciortino<sup>°</sup> and Piero Tartaglia<sup>°</sup>

<sup>+</sup> Institute of Physics, Johannes-Gutenberg University, D-55099 Mainz, Germany

<sup>†</sup>Département de Physique des Matériaux, Université Claude Bernard and CNRS, 69622 Villeurbanne Cedex, France

<sup>°</sup> Dipartimento di Fisica and Istituto Nazionale per la Fisica della Materia, Università di Roma *La Sapienza*, P.le Aldo Moro 2, I-00185 Roma, Italy.

**Abstract** Using molecular dynamics computer simulations we investigate the out-of-equilibrium dynamics of a Lennard-Jones system after a quench from a high temperature to one below the glass transition temperature. By studying the radial distribution function we give evidence that during the aging the system is very close to the critical surface of mode-coupling theory. Furthermore we show that two-time correlation functions show a strong dependence on the waiting time since the quench and that their shape is very different from the one in equilibrium. By investigating the temperature and time dependence of the frequency distribution of the normal modes we show that the energy of the inherent structures can be used to define an effective (time dependent) temperature of the aging system.

## 1 Introduction

In the last few years ample evidence has been accumulated that the mode-coupling theory of the glass transition (MCT) gives a reliable description of the dynamics of simple supercooled liquids on a qualitative as well as quantitative level [1]. Recently it has even been documented that also some aspects of the dynamics of *strong* glass formers are described well by the theory [2]. Thus we can conclude that many of the key aspects of the dynamics of supercooled liquids are understood in a quite satisfactory way. This is not yet the case for the dynamics of glasses *below* the glass transition temperature, i.e. in that temperature regime in which the *equilibrium* relaxation time significantly exceeds the time scale of the experiment. Only relatively recently first attempts have been made to understand this out-of-equilibrium dynamics within the framework of statistical mechanics and thermodynamics [3]. In particular it was found that, for certain systems, the equations of motion describing the dynamics below  $T_g$  are formally quite similar to the MCT equations, which, as discussed above, describe well the relaxation dynamics *above*  $T_g$ . Whether or not these out-of-equilibrium theories will be equally successful to describe the dynamics of structural glasses below  $T_g$  is currently

---

<sup>1</sup>Talk presented at “Unifying Concepts in Glass Physics”, ICTP, Trieste 15 - 18 September 1999

not known and in the present paper we discuss some computer simulations which have been done to test these theories.

## 2 Model and Details of the Simulations

The system we consider is a binary (80:20) mixture of particles which interact with a Lennard-Jones potential,  $V_{\alpha\beta} = 4\epsilon_{\alpha\beta}[(\sigma_{\alpha\beta}/r)^{12} - (\sigma_{\alpha\beta}/r)^6]$ . Here  $\alpha, \beta \in \{A, B\}$  denote the species of the particles and the parameters  $\epsilon_{\alpha\beta}$  and  $\sigma_{\alpha\beta}$  are given by  $\epsilon_{AA} = 1.0$ ,  $\sigma_{AA} = 1.0$ ,  $\epsilon_{AB} = 1.5$ ,  $\sigma_{AB} = 0.8$ ,  $\epsilon_{BB} = 0.5$ , and  $\sigma_{BB} = 0.88$ . This potential is truncated and shifted at a distance  $\sigma_{\alpha\beta}$ . In the following we will use  $\sigma_{AA}$  and  $\epsilon_{AA}$  as the unit of length and energy, respectively (setting the Boltzmann constant  $k_B = 1.0$ ). Time will be measured in units of  $\sqrt{m\sigma_{AA}^2/48\epsilon_{AA}}$ , where  $m$  is the mass of the particles.

The equations of motions have been integrated with the velocity form of the Verlet algorithm, using a step size of 0.02. The number of A and B particles were 800 and 200, respectively and the size of the box was  $(9.4)^3$ .

In the past the *equilibrium* dynamics of this system has been determined in great detail [4, 5]. In particular it was shown that at low temperatures the relaxation dynamics is described very well by MCT with a critical temperature of  $T_c = 0.435$ . To investigate the aging dynamics we therefore equilibrated the system at the high initial temperature  $T_i = 5.0$  and quenched it at time zero to a final temperature  $T_f \in \{0.1, 0.2, 0.3, 0.4, 0.435\}$ . This quench was done by coupling the particles every 50 time steps to a stochastic heat bath which was kept on during the subsequent propagation of the system at low (kinetic) temperature. In order to improve the statistics of the results we averaged over 8-10 different realizations of the system.

## 3 Results

Within the framework of the idealized version of MCT the aging process is viewed as a slow approach of the system to the so-called “critical surface” of MCT. This surface is a hyper-surface in the parameter space of the coupling constants, which in the case of a structural glass are given by the magnitude of  $S(q)$ , the static structure factor at wave-vector  $q$ , and divides this space into a region in which the system is liquid-like and one in which it is solid-like, i.e. a glass. (In order to avoid some mathematical subtleties we consider only a discrete and finite set of wave-vectors, thus the parameter space is finite dimensional.) In order to check whether or not this surface does indeed have any relevance for the aging dynamics of our system we calculated the time dependence of  $g_{AA}(r)$ , the radial distribution function between two A particles, a quantity which is closely related to the static structure factor. In Fig. 1 we show  $g_{AA}$  for different times  $t$  after the quench (main figure). From this graph we see that immediately after the quench the function changes rapidly (compare the curves for  $t = 0$  and  $t = 10$ ) but soon afterwards

shows only a very weak time dependence and then can soon be considered as constant within the accuracy of the data. That this limiting curve depends on the final temperature  $T_f$  of the quench is shown in the inset of the figure, where we show  $g_{AA}(r)$  for other values of  $T_f$ . We see that with decreasing  $T_f$  the height of the main peak increases and that its width decreases. The reason for this is that at such low temperatures the particles vibrate in the cages formed by their neighbors and that the size of this cage decreases with decreasing temperature. Note that this dependence demonstrates that for different values of  $T_f$  the system populates states in different regions in configuration space.

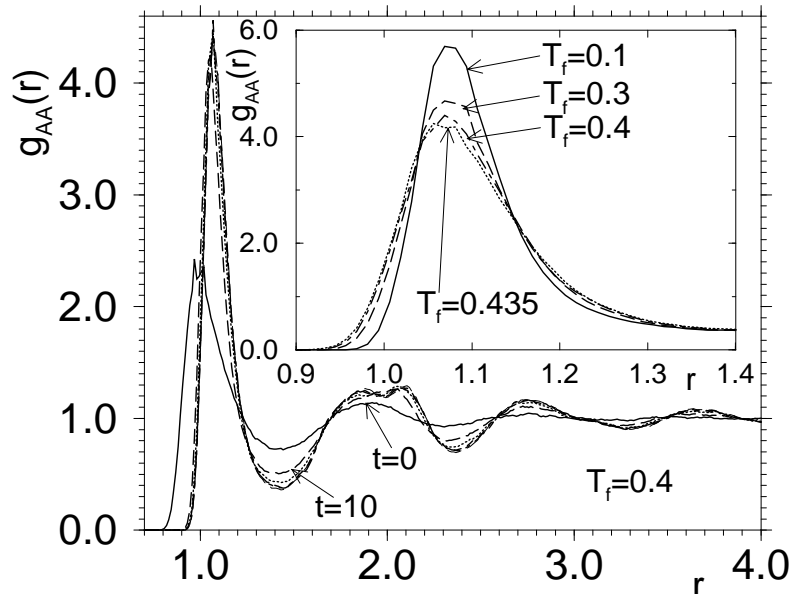


Figure 1: Main figure: radial distribution function between the A particles for different times for  $T_f = 0.4$ . The times are  $t = 0$ , i.e. before the quench,  $t = 10, 100, 1000, 10000$ , and  $63100$  time units. Inset: The same quantity at  $t = 63100$  for different values of  $T_f$ .

If the view put forward by MCT is correct these states should all be close to the critical surface discussed above. In order to check this prediction we calculated the area under the first peak in  $g_{AA}(r)$ . This area is roughly proportional to the height of the main peak in the static structure factor and previous calculations have shown [6, 7] that for simple systems such as the present one this is the most relevant coupling parameter, i.e. the most relevant direction in the parameter space of the coupling constants. In Fig. 2 we show this area  $c(t)$  for the different temperatures  $T_f$ , i.e.  $c(t) = 4\pi \int_0^{r_c} r^2 g_{AA}(t) dr$ , where  $r_c$  is the location of the minimum between the first and second peak in  $g_{AA}(r)$ . (Note that  $c$  is nothing else than the average number of A particles that surround an A particle.). The different symbols correspond to times 0, 10, 40, 60, 100, 160, 250, 400, 630, 1000, 1580, 2510, 3980, 6310, 10000, 15850, 25120, 39810, and 63100 and are thus

space roughly equidistant on a logarithmic time axis. (In order to expand the axis at low temperatures we chose a logarithmic temperature scale.) From the main figure we recognize that at the beginning the area does indeed depend strongly on time that, however, at intermediate and long times  $c(t)$  is essentially constant within the noise of the data (see inset). We see that within the time scale covered the value of  $c(t)$  changes only by about 6%.

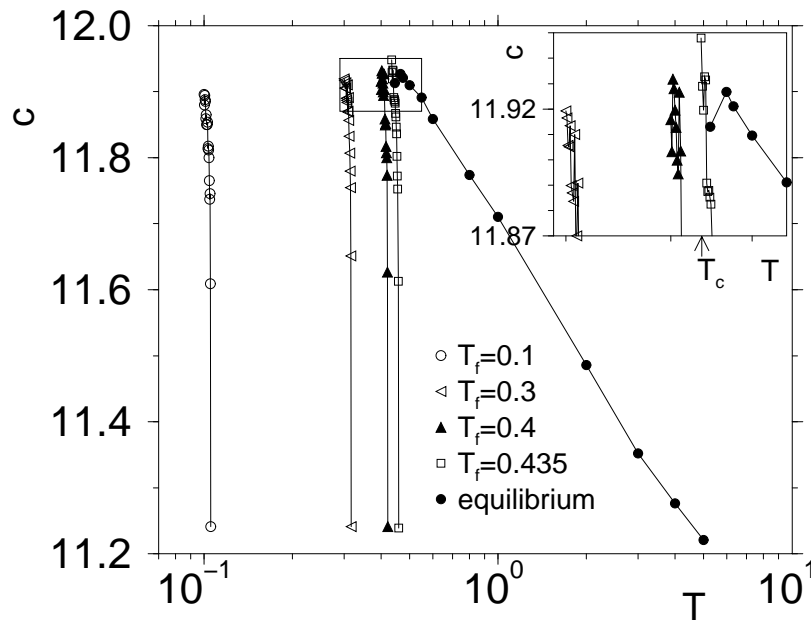


Figure 2: Main figure: time dependence of the area under the first peak in  $g_{AA}(r)$  for different values of  $T_f$ . The right-most curve is the same quantity for the *equilibrium* case. Inset: enlargement of the equilibrium curve around the critical temperature of MCT.

That this small change is nevertheless very significant is demonstrated by the right-most curve (filled circles) in which the *equilibrium* value of  $c$  at different temperatures is shown [4, 13]. From that curve we see that in the temperature range  $5.0 \geq T \geq 0.446$  the area changes also only by about 6%, despite the fact that the dynamics of the system slows down by about five orders of magnitude [4].

The most relevant information from this graph is that the value of  $c(t)$  at long times seems to be almost independent of  $T_f$ , thus giving evidence that at these times the system is indeed close to the critical surface of MCT. That this is indeed the critical surface can be seen from the inset where we show an enlargement of the equilibrium curve at low temperatures. From previous investigations we know that at these temperatures the (equilibrium) system is very close to its critical temperature and that therefore the values of  $c$  of the equilibrium curve are very close to the critical ones and which are around 11.93. From the inset we recognize that also the long time values of  $c(t)$  are very close to this number which is thus evidence that also the aging systems are, at long times, quite close to the critical surface. A careful inspection of

the main figure reveals, however, that the curves for low values of  $T_f$  are a bit below this critical value, an observation which we will discuss below.

From Figs. 1 and 2 we see that during the aging process the time dependence of the radial distribution function is rather weak. This situation is typical for so-called “one-time quantities”, i.e. observables which *in equilibrium* are constant. (Below we will discuss exceptions to this trend.) A much stronger time dependence is found for the so-called “two-time quantities”, i.e. the generalizations of the equilibrium time correlation functions to the case of the out-of equilibrium case. In equilibrium a time auto-correlation function of an observable  $y(t)$  depends only on the time difference, i.e.  $\langle y(t_w)y(t_w + \tau) \rangle = \langle y(\tau)y(0) \rangle$ , where  $\langle \cdot \rangle$  is the thermodynamic average. This equality no longer holds for the out-of equilibrium case, since due to the generation of the out-of equilibrium situation the time-translation invariance of the system is lost. Therefore it is necessary to keep track of both times,  $t_w$ , the time since the quench, and  $\tau$ , the time since the start of the measurement. In the following we will study the case that the observable is  $\rho_s(k, t)$ , the space-Fourier transform of the density of a tagged at wave-vector  $k$ . This quantity is related to the positions of the particles via

$$\delta\rho(k, t) = \frac{1}{N} \sum_{j=1}^N \exp[i\mathbf{k} \cdot \mathbf{r}_j(t)] \quad . \quad (1)$$

In equilibrium the resulting time correlation function is the so-called incoherent intermediate scattering function  $F_s(k, t) = \langle \rho(k, t)\rho(-k, 0) \rangle$  which can be measured in scattering experiments. For the out-of equilibrium case we generalize this to

$$C_k(t_w + \tau, t_w) = \frac{1}{N} \sum_j \exp[i\mathbf{k} \cdot (\mathbf{r}_j(t_w + \tau) - \mathbf{r}_j(\tau))] \quad (2)$$

(Note that these last equations are trivially generalized to multi-component systems.) In Fig. 3 we show the  $\tau$  dependence of  $C_k(t_w + \tau, t_w)$  for the A particles for different waiting times  $t_w$ . The value of the wave-vector is  $k = 7.23$ , the location of the main peak in the structure factor for the A-A correlation. (Other values of  $k$ , as well as the curves for the B particles look qualitatively similar.) From this figure we recognize that this time correlation function shows a very strong waiting time dependence, thus showing that the investigation of aging effects is much easier when one considers two-time quantities instead of one-time quantities (Figs. 1 and 2). Note that this waiting time dependence is not found at short times  $\tau$ , *if  $t_w$  is large*, in that in this time regime the different curves collapse onto a master curve. In this time regime the particles are still inside the cage formed by their neighbors and thus we conclude from the figure that this vibrational motion becomes independent of the waiting time, if the latter is large. In Ref. [8] evidence was given that the approach of the curves to the plateau is given by a power-law, in agreement with the mean-field theories.

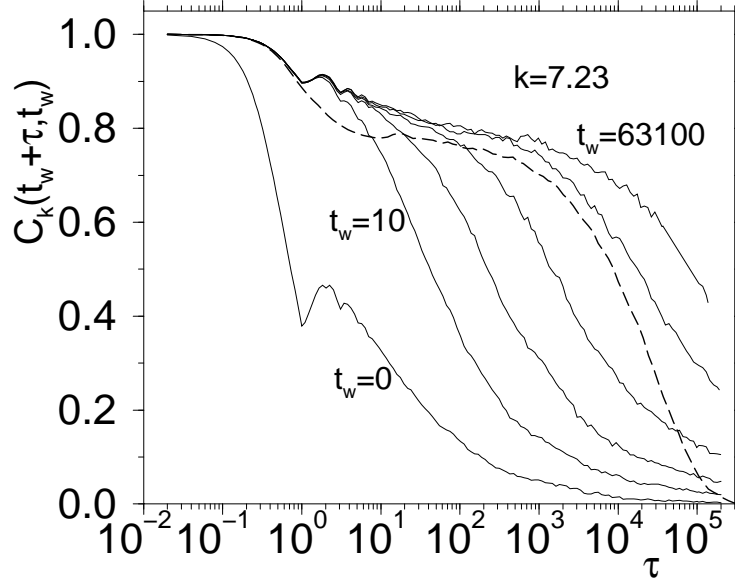


Figure 3: Time dependence of the generalization of the incoherent intermediate scattering function to the out-of-equilibrium case. The different curves correspond to different waiting times.  $T_f = 0.4$ . The dashed curve is the *equilibrium* curve at 0.446.

For larger times  $\tau$  the particle starts to leave the mentioned cage (the correlator starts to fall below the quasiplateau at intermediate times) and from the figure we see that the time at which this happens increases with increasing  $t_w$  in that the time scale for the second relaxation step increases rapidly with  $t_w$ . As it has been demonstrated elsewhere [9], this relaxation times scales roughly like  $t_w^{0.9}$ , i.e. it shows a sub-aging behavior.

Also included in Fig. 3 is the *equilibrium* curve at  $T = 0.446$  for the same wave-vector. Comparing this curve with the out-of-equilibrium curves for large  $t_w$  shows that the height of the plateau is very similar. What is, however, very different is the *second* relaxation process in that the equilibrium curve decays much more rapidly, i.e. has a larger slope, than the aging curves. A detailed analysis shows that the former curve is approximated well by a Kohlrausch-Williams-Watts function [4],  $\exp(-(\tau/\tau_0)^\beta)$  whereas the latter curves are power-laws, with an exponent that depends on  $k$  but not on the waiting time [8, 10].

The curves in Fig. 3 are for the final temperature  $T_f = 0.4$ , i.e. just about 10% below the critical temperature of MCT ( $T_c = 0.435$ ). In order to see how  $T_f$  affects the relaxation we show in Fig. 4 the same type of correlation function as in Fig. 3, but this time for  $T_f = 0.1$ . Although the overall behavior of these curves are similar to the ones for the higher  $T_f$  some significant differences are found. First of all we see that the height of the plateau,  $f_c(k)$ , is now quite a bit larger than the one for  $T_f = 0.4$ . This change can easily be understood by recalling that for short times the motion

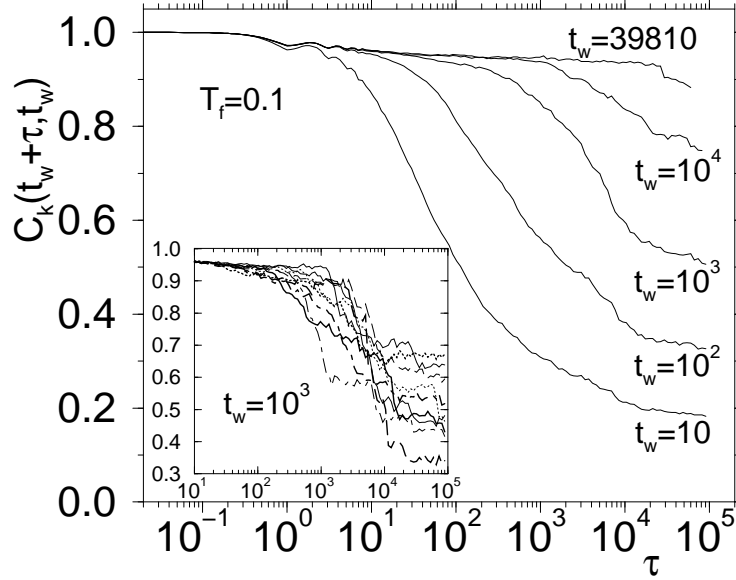


Figure 4: Time dependence of the generalization of the incoherent intermediate scattering function to the out-of-equilibrium case for  $T_f = 0.1$

of the particles is dominated by their rattling inside the cage. To a first approximation this rattling can be described by a superposition of harmonic oscillators and thus their amplitude will be proportional to  $T_f$ . Thus we expect that  $1 - f_c(k)$  is proportional to  $T_f$ , and an inspection of the curves in Figs. 3 and 4 shows that this is indeed the case. More noteworthy is the observation that for large  $t_w$  the curves seem to show a second plateau at long times, which seems not to be present for  $T_f = 0.1$ .

In order to understand the origin of this second plateau it is useful to look at the individual runs for  $T_f = 0.1$ , which are shown for  $t_w = 10^3$  in the inset of Fig. 4. From this inset we see that the different curves show a relatively sharp drop in the time range  $2 \times 10^2 \leq \tau \leq 2 \times 10^4$  and then is almost constant. Note that the time at which this drop occurs depends on the realization. A careful analysis of the configurations just before and after a sudden drop shows that this fast relaxation is related to a very cooperative motion of about 10% of the particles [8]. Thus it seems that this mechanism is the most effective way to release the stress that is in the configuration due to the quench. This is in contrast to the behavior at higher values of  $T_f$  in that there the stress is smaller and thus the system can remove it in a more gradual way, i.e. without the occurrence of the “earthquakes” that are seen at the lower temperatures.

In the remaining part of the paper we will discuss the aging of the system from the point of view of the configuration space. For this we make use of the concept of the “inherent structure” (IS), which was introduced some time ago by Stillinger and Weber [11] and can be described as follows: Any point in configuration space can be used as the starting point of a steepest descent

procedure in the potential energy of the system. The endpoint of this steepest descent is the IS for the starting point. Thus in this way the configuration space can be decomposed uniquely into the basins of attractions of the IS (apart from some points of measure zero). By focusing on the IS we therefore can study the evolution of the system during the aging process without being disturbed by the vibrational part of the particle motion.

In Fig. 5 we show the temperature dependence of  $e_{\text{IS}}$  the potential energy of the system in the IS *in equilibrium*, Fig. 5a (see also Ref. [5]). We recognize that at high temperatures  $e_{\text{IS}}$  is basically constant and starts to decrease quickly below  $T \approx 1.0$  which shows that the energy landscape, as characterized by the height of the local minima, starts to change only when the system enters the supercooled regime. In Fig. 5b we show the *time* dependence of  $e_{\text{IS}}$  for the different final temperatures investigated. We see that the curves for small  $T_f$  show three regimes. (Although the curves with higher  $T_f$  show only two regimes we will argue below that also they should show a third regime if one would be able to simulate for longer times.) The first regime is observed at short times and in it  $e_{\text{IS}}(t)$  is essentially independent of time. After this time regime  $e_{\text{IS}}(t)$  enters the second regime during which the system is able to decrease its energy. After a certain time  $e_{\text{IS}}$  crosses over to a weaker time dependence and thus the system enters the third regime.

In order to understand these two last time regimes it is useful to recall some results which have been obtained by analyzing the instantaneous normal modes of supercooled liquids *in equilibrium* [12]. Although these results have been obtained for supercooled water it is likely that they can be transferred to the present systems as well. What has been shown in Ref. [12] is that the number of modes that lead the system to a *new* local minimum decreases with decreasing temperatures and vanishes at the MCT temperature  $T_c$ . Thus we can say that for temperatures above  $T_c$  the typical configuration of the system has at least one unstable mode, i.e. direction of motion, whereas for temperatures below  $T_c$  the system mainly sits in the vicinity of a local minimum, i.e. oscillates around a metastable location. Thus at  $T_c$  the system has a thermal energy which is comparable with the difference in energy between  $e_{\text{IS}}(T_c)$  and the lowest lying saddle point leading to a neighboring minimum. Hence, for temperatures below  $T_c$  the dynamics of the system becomes dominated by activated processes. Note that the fact that the temperature dependence of the relaxation dynamics shows a strong deviation from an Arrhenius temperature dependence [4, 14] implies that the height of the *effective* barrier between two minima is not constant but increases with decreasing temperature and, as explained above, at  $T_c$  this barrier is on the order of  $T_c$ .

All this holds for the equilibrium case. For the out-of-equilibrium case the situation is qualitatively similar but there is the important difference that now the system has only the thermal energy  $T_f$ . The three regimes seen in Fig. 5 can thus be explained as follows. In the first regime the typical configurations of the system are still quite similar to the ones found *in*



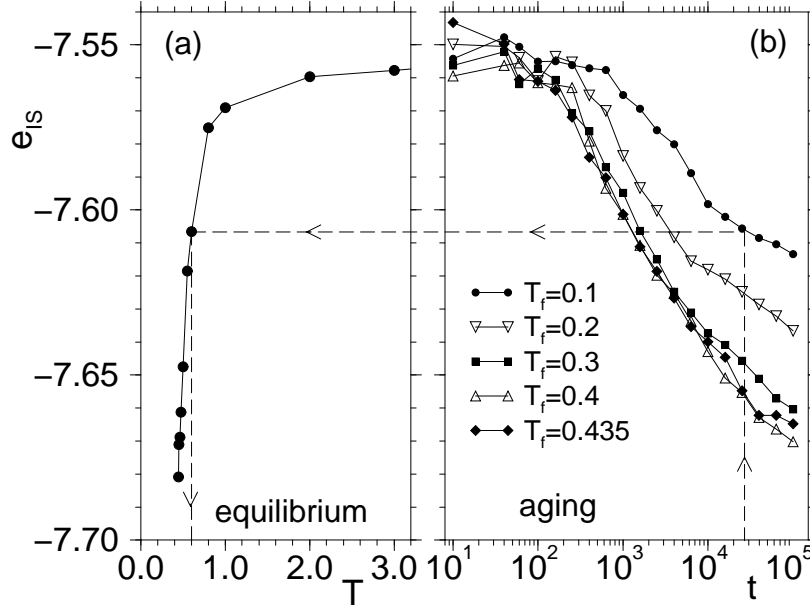


Figure 5: Time and time dependence of the energy of the IS. a): equilibrium, b) out-of-equilibrium. Reproduced from Ref. [15].

*equilibrium* at high temperatures, i.e. close to the initial temperature. In this part of configuration space the effective barriers between adjacent minima are relatively small but nevertheless noticeable. Since it takes the system some time to find configurations with lower energy,  $e_{\text{IS}}$  does not decrease. Only after some time the system manages to find configurations which are energetically more favorable and hence  $e_{\text{IS}}$  starts to decrease, i.e. in Fig. 5  $e_{\text{IS}}(t)$  enters the second regime. The time until such better configurations are found increases with decreasing  $T_f$ , since a smaller kinetic energy makes it harder for the system to cross the barriers.

During the aging process the system will lower its energy and start to explore configurations which, *in equilibrium*, correspond to lower and lower temperatures. After some time it will have reached that part of configuration space in which the effective barriers to cross from one minimum to the neighboring one have a height  $k_B T_f$  and thus the relaxation mechanism will change to an activated process. Since this type of relaxation is less efficient than the one in which the system still finds unstable modes, the rate by which the energy decreases is decreasing. Thus the  $e_{\text{IS}}(t)$  curve shows a bend, which can be seen in Fig. 5 when the system is entering the third regime. Note that this bend in the  $e_{\text{IS}}(t)$  curves should occur at a value of  $e_{\text{IS}}$  which increases with decreasing  $T_f$  and this is exactly what is seen in Fig. 5. In particular we expect from the reasoning above that if  $T_f$  is very close to  $T_c$  the third regime should hardly be visible, and this expectation is indeed supported by Fig. 5.

Since  $e_{\text{IS}}$  seems to be a quite sensitive quantity to locate the place of the system in configuration space, and this is in contrast to most other one-time

quantities, we can use it to define an effective temperature  $T_e(t)$  during the aging process. For this we read off the value of  $e_{\text{IS}}(t)$  of the aging system at a time  $t$ , and define  $T_e(t)$  to be that temperature  $T$  at which the system *in equilibrium* has the same value of  $e_{\text{IS}}$  (see Fig. 5). In order to check whether this definition of  $T_e(t)$  has any physical meaning it is necessary to show that from the knowledge of  $T_e(t)$  it is possible to calculate other properties of the aging system. One such property is e.g. the distribution of the frequencies of the normal modes of the system. We have done this and found [15] that the value of  $T_e(t)$  does indeed allow to calculate this distribution. In the present paper we show, however, only  $\bar{\nu}$ , the first moment of this distribution (see Fig. 6) since it has a better statistical accuracy than the distribution itself.

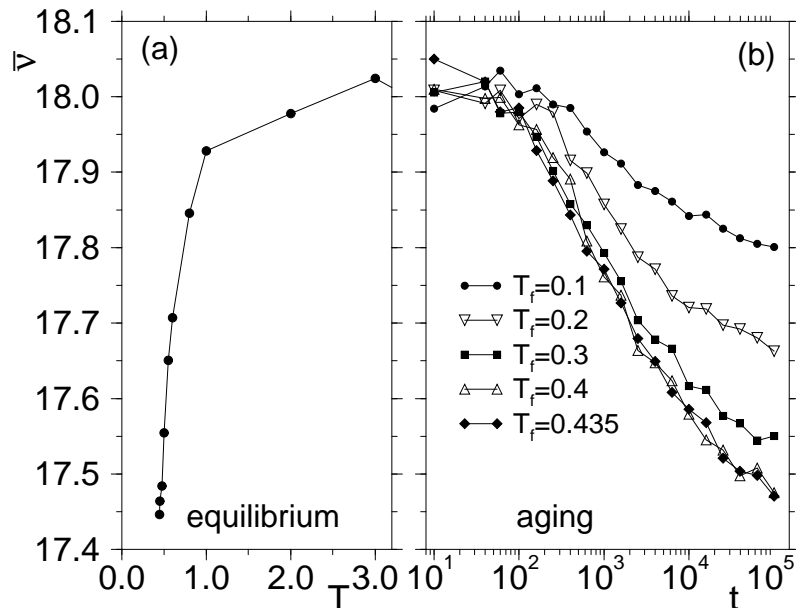


Figure 6: Time and time dependence of the first moment of the normal mode spectrum. a): equilibrium, b) out-of-equilibrium. Reproduced from Ref. [15].

In Fig. 6 we show  $\bar{\nu}$  for the equilibrium case as well as the aging case (left and right panel, respectively). A comparison of these curves with the one for  $e_{\text{IS}}$  in Fig. 5 shows immediately that the two sets of curves are very similar. Hence it follows that  $T_e(t)$  can indeed be used to predict some of the properties of the aging system and thus can indeed be considered as an effective temperature.

## 4 Summary and Conclusions

We have investigated the properties of a simple glass former after a quench from a high temperature to a low temperature. From the radial distribution function we have evidence that for long times after the quench the system is

very close to the critical surface of the MCT. Note that, since this surface can be calculated from the structure factor, it will *in the out-of-equilibrium situation* be a function of  $T_f$ , since  $S(q)$  does not only depend on the IS but also on the thermal broadening of this configuration. This is the explanation why during the aging the system is “stuck” in parts of configuration space that depend on the value of  $T_f$ . At long times typical configurations have the property that if their IS is thermally broadened with a temperature  $T_f$  the resulting structure factor is very close to the critical surface of the MCT equations. Following the conclusions of Ref. [12] one can rephrase this by saying that for these configurations the typical barrier which leads to a neighboring minimum is on the order of  $T_f$ .

Finally we mention that in a different place we have shown that the IS can be used to determine the configurational entropy of the system at low temperatures [16] which in turn allows to calculate such interesting quantities as the Kauzmann temperature.

Acknowledgments: We thank L. Cugliandolo, J. Kurchan, and A. Latz for many helpful discussions. This work was supported by the Pole Scientifique de Modélisation Numérique at ENS-Lyon, and the Deutsche Forschungsgemeinschaft through SFB 262.

## References

- [1] W. Götze, J. Phys.: Condens. Matter **11**, A1 (1999).
- [2] T. Franosch, W. Götze, M. R. Mayr, and A. P. Singh, Phys. Rev. E **55**, 3183 (1997); J. Horbach and W. Kob, Phys. Rev. B **60**, 3169 (1999); (unpublished).
- [3] S. Ciuchi and F. de Pasquale, Nuclear Physics B **300**, 31 (1988); L. F. Cugliandolo and J. Kurchan, Phys. Rev. Lett. **71**, 173 (1993); L. F. Cugliandolo, J. Kurchan, and G. Parisi, J. Phys. I (France) **4**, 1641 (1994); J. P. Bouchaud and D. S. Dean, J. Phys. I (France) **5**, 265 (1995); J. Kurchan and L. Laloux, J. Phys. A, **29**, 1929 (1996); C. Monthus and J.-P. Bouchaud, J. Phys. A: Math. Gen. **29**, 3847 (1996); J.-P. Bouchaud, L. F. Cugliandolo, J. Kurchan, and M. Mézard, p. 161 in *Spin Glasses and Random Fields*, Ed.: A.P. Young (World Scientific, Singapore, 1998). Th. M. Nieuwenhuizen, Phys. Rev. Lett. **80** 5580 (1998); preprint cond-mat/9807161, and references therein, A. Latz (unpublished)
- [4] W. Kob and H. C. Andersen, Phys. Rev. Lett. **73**, 1376 (1994); Phys. Rev. E **51**, 4626 (1995); *ibid.* **52**, 4134 (1995).
- [5] S. Sastry, P. G. Debenedetti, and F. H. Stillinger, Nature **393**, 554 (1998).

- [6] U. Bengtzelius, W. Götze and A. Sjölander, J. Phys. C **17**, 5915 (1984).
- [7] M. Nauroth and W. Kob. Phys. Rev. E, **55**, 657 (1997).
- [8] W. Kob and J.-L. Barrat, Eur. Phys. J. B (1999) (in press).
- [9] W. Kob and J.-L. Barrat, Phys. Rev. Lett. **78**, 4581 (1997).
- [10] W. Kob and J.-L. Barrat, Physica A **263**, 234 (1999).
- [11] T. A. Weber and F. H. Stillinger, Phys. Rev. B **31**, 1954 (1985); F. H. Stillinger, Science, **267** 1935 (1995).
- [12] F. Sciortino and P. Tartaglia, Phys. Rev. Lett. **78**, 2385 (1997).
- [13] T. Gleim, W. Kob, and K. Binder, Phys. Rev. Lett. **81**, 4404 (1998).
- [14] P. Gallo, F. Sciortino, P. Tartaglia and S.-H. Chen, Phys. Rev. Lett. **76**, 2730 (1996); S.-H. Chen, P. Gallo, F. Sciortino, and P. Tartaglia, Phys. Rev. E **56** 4231 (1997); F. Sciortino, L. Fabbian, S.-H. Chen, and P. Tartaglia, Phys. Rev. E **56** 5397 (1997).
- [15] W. Kob, F. Sciortino, and P. Tartaglia, preprint cond-mat/9905090.
- [16] F. Sciortino, W. Kob, and P. Tartaglia, Phys. Rev. Lett. **83**, 3214 (1999).